

Resonant Inelastic X-ray Scattering of Tantalum Double Perovskite Structures

Ju Hyun Oh¹, Jung Ho Kim², Jung Hyeon Jeong¹, Seo Hyoung Chang^{1,3*}

¹Department of Physics, Pukyong National University, Busan 48513, South Korea

²Advanced Photon Source, Argonne National Laboratory, Lemont 60439, United States

³Department of Physics, Chung-Ang University, Seoul 06974, South Korea

* e-mail: cshyoung@pknu.ac.kr and cshyoung@cau.ac.kr

In this paper, we investigated electronic structures and defect states of SrLaMgTaO₆ (SLMTO) double perovskite structures by using resonant inelastic x-ray scattering. Recently, Eu³⁺ doped SLMTO red phosphors have been intensively investigated due to their higher red emission efficiency than commercial white light emitting diodes (W-LED). However, understanding on the electronic structures and defect states of host SLMTO compounds, which are specifically related to the W-LED and photoluminescence (PL), is far from complete. Here, we found that the PL spectra of SLMTO powder compounds sintered at higher temperature, 1400°C, were weaker in the blue emission regions (at around 400 nm) and enhanced in near infrared (NIR) regions, compared to those sintered at 1200°C. To elucidate the difference of the PL spectra, we performed x-ray diffraction with Rietveld refinements, energy-dispersive x-ray spectroscopy, x-ray absorption spectroscopy, and resonant inelastic x-ray spectroscopy at Ta L-edge.

Keywords: Resonant Inelastic X-ray Scattering, SrLaMgTaO₆, Double Perovskites, Light Emitting Diodes

1. Introduction

Although white light emitting diodes (W-LEDs) were realized by using a yellow phosphor (YAG:Ce) coated on the blue LED chips, this white light makes us uncomfortable due to the deficiency of the red light (above 600 nm) [1-5]. To overcome the drawbacks, many researchers have intensively investigated and developed the red phosphors having high efficiency and chemical stability. Of the many red phosphors, Eu^{3+} doped SrLaMgTaO_6 red phosphors have been reported to emitting a higher red emission efficiency than the commercial $\text{Y}_2\text{O}_3:\text{Eu}^{3+}$ red phosphors [6,7]. Nevertheless, few studies on the relationship between the photoluminescence (PL) properties, electronic structures, and defect states of SrLaMgTaO_6 (SLMTO) host lattice have been found.

The crystal structure of bulk SLMTO is monoclinic and a double perovskite structure of formula $\text{AA}'\text{BB}'\text{O}_6$ [8,9]. The physical and chemical properties of perovskite compounds are closely related to the oxygen vacancies, cation stoichiometry, the configuration of the A and/or B cations, octahedral rotations [10,11]. For instance, small oxygen vacancies or cation stoichiometry can induce different electronic structures and defect states of the SLMTO compounds. However, our understanding on the relationship between the photoluminescence (PL) spectra and specific defect states in the SLMTO compounds is very poor. Therefore, monitoring oxygen vacancies or element-specific defects in the compounds can give a direct clue to unveil the microscopic origin of PL spectra.

Resonant inelastic x-ray scattering (RIXS) is a powerful tool to monitor the change of defect states related to the elements in SLMTO compounds [12]. As a photon-in and photon-out, RIXS at the Ta L_3 -absorption edge (9.881 keV) is a good candidate for verifying electronic excitation in Tantalum double perovskite compounds in the non-destructive way. Ta ion in stoichiometric SLMTO has 5+ valency and 5d orbitals are fully unoccupied ($5d^0$). When oxygen vacancies near Ta ions exist, 5d orbitals were changed from unoccupied to partially occupied states. Then, we propose that RIXS at Ta L_3 -absorption edge can detect and verify Ta 5d-related defect states inside the band gap of SLMTO.

In this letter, we investigated structural, electronic excitation, and photoluminescence (PL) properties of SrLaMgTaO_6 powder compounds, which were sintered at 1200°C and 1400°C, respectively. X-ray diffraction measurements with Rietveld refinement analyses indicated that the two

samples had the same monoclinic structure but showed small changes of the lattice parameters less than 0.2 %. As increasing the sintering temperature, the strong red-to-NIR emission band is observed. Our resonant inelastic x-ray scattering (RIXS) studies clearly demonstrate that there are significant changes in the RIXS spectra, indicating little Ta-related oxygen vacancies in the SLMTO compounds. The findings of this study are expected to contribute the development of higher-efficiency double-perovskite phosphors, as they reveal the relation between PL characteristics and Ta-related defects of the double-perovskite host lattices.

2. Experimental methods

Polycrystalline ceramic samples with composition of SrLaMgTaO_6 (SLMTO) were synthesized by a conventional mixed oxide method employing the solid-state reaction of SrCO_3 (99.994%), La_2O_3 (99.99%), $(\text{MgCO}_3)_4\text{Mg}(\text{OH})_2 \cdot 5\text{H}_2\text{O}$ (99.99%), and Ta_2O_5 (99.99%). All the reagents were purchased from Alfa-Aesar. The mixture of starting materials was mixed and ground in an agate mortar, then was calcined at 900°C for 2 hr. After that, the mixture was ground again, and sintered 1200°C and 1400°C for 12hr, respectively.

The crystal structures were analyzed using experimental X-ray diffraction (XRD) data and Rietveld refinement software (general structure analysis system, GSAS). XRD data were collected in the range of $10\text{--}80^\circ$ for a scan speed of $2^\circ/\text{min}$ using the X'Pert-MPD system (Panalytical, Netherland) with $\text{Cu K}\alpha_1$ radiation at a wavelength of 1.5406 \AA . Energy-dispersive spectroscopy (EDS, HORIBA) attached to a scanning electron microscope (SEM, S-2700, HITACHI) was used for chemical composition analysis. The photoluminescence (PL) spectra were measured at room temperature and recorded with a fluorescence spectrophotometer (Acton SpectraPro 750-Triplet Grating Monochromator) from a charge-coupled device (CCD) detector (Princeton EEV 10241024 and PI-Max 133 controller). Resonant inelastic x-ray scattering (RIXS) and x-ray absorption spectroscopy (XAS) experiments were performed at the 27 ID beamline of Advanced Photon Source, Argonne National Laboratory. The details for RIXS measurements are presented elsewhere [13].

3. Results and discussions

The crystal structures of polycrystalline SLMTO powder samples were characterized by XRD θ - 2θ scan measurements. As shown in Fig. 1(a), we synthesized and measured the XRD patterns of SLMTO samples sintered at different temperatures, 1200°C and 1400°C, respectively. Based on monoclinic structure with space group P21/n in the inorganic crystal structure database (ICSD), we performed Rietveld refinement analyses. As shown in Table I, the R factors (3 – 6 %) of both samples are reasonable and similar values, which are related to the quality and reliability of the fitting results [14-16]. The lattice parameters and volume of the sample sintered at different temperatures were very slightly changed less than 0.2 %; as increasing the sintering temperature, the lattice constant of a decreases while the b and c values increases.

As shown in Fig. 1(b), the Sr^{2+} and La^{3+} ions can be randomly distributed on A site, and they are usually surrounded by twelve oxygen ions, but there are eight oxygen ions around the A site in this monoclinic system and four oxygen ions are away from the A site (approximately above 0.3 nm) [17]. The Mg^{2+} and Ta^{5+} are orderly located in the B site with the oxygen octahedral surrounded by six oxygen ions. Most double-perovskite compounds have octahedral tilting distortion due to the mismatch between the ionic radius. The degree of the octahedral tilting distortion can be explained by tolerance factor (t). The t value of SLMTO is 0.952, calculated by the following relation,

$$t = (r_{\text{Sr}} + r_{\text{O}}) / \sqrt{2}(r_{\text{Mg,Ta}} + r_{\text{O}}) \quad \text{Eq. (1)}$$

where r is the composition weighted ion radius at the given site and $r_{\text{Mg,Ta}}$ is the average ionic radius of Mg^{2+} and Ta^{5+} ions. The SLMTO compounds have t value smaller than 1, and thus octahedral tilting becomes favored and the $a^-a^-c^+$ tilting is observed in SLMTO compound [8]. Owing to the small change of lattice parameters in the two samples, the octahedral tilting patterns can be maintained.

To check the possibilities of stoichiometry and morphology issues in the samples, we performed the energy-dispersive x-ray spectroscopy (EDS) as shown in Fig. 2. The EDS results showed the presence of strontium (Sr), lanthanum (La), magnesium (Mg) and tantalum (Ta). Specifically, there are no other

contaminated elements in both of SLMTO powder samples. The inset of Fig. 2(a) and Fig. 2(b) displays the SEM images of SLMTO powders sintered at 1200°C and 1400°C, respectively. The crystal morphology and the particle size in both of SLMTO powders can be varied with different sintering temperature; the SLMTO powder sample sintered at 1400°C exhibits the larger particle size than those of the sample sintered at 1200°C.

To investigate the sintering temperature effects on the LED, we performed the PL spectra of SLMTO powder samples using a Nd:YAG laser as excitation source, as shown in Fig. 3(a). Under the excitation of 266 nm, the SLMTO powder samples with different sintering temperatures drastically show the different PL spectra. For instance, the SLMTO powders sintered at 1200°C have a strong and broad emission band centered at 405 nm and weak emission band centered at approximately 700 nm, compared to that of the sample sintered at 1400°C. In other words, the strong emission centered at 405 nm is weakened as increasing the sintering temperature, while the emission band in NIR region (close to the red light) is enhanced.

To get further insight on the physical origin of the emissions in the two regimes, we fitted the PL spectra of SLMTO powder samples, as shown in Fig. 3(b) and Fig. 3(c). Note that the peak at 532 nm ($\sim 18796 \text{ cm}^{-1}$) marked with an asterisk was excluded from Gaussian curve fitting because it is the second harmonic peak of Nd:YAG laser. Firstly, the broad emission band centered at 405 nm in the blue emission region is systematically decomposed into three components (peak A, B, and C) in both samples. Interestingly, the intensities of peak A and B are nearly similar in both samples, but the C component centered at 425 nm ($\sim 23480 \text{ cm}^{-1}$) shows quite different PL intensity depending on the samples. With the increase of the sintering temperature, the intensity of peak C is suppressed more than 10 times. Secondly, Fig. 3(b) and Fig. 3(c) clearly shows that the NIR emission is enhanced (D and E components). Especially, new emission peaks are observed, which is denoted by F and G components in Fig. 3(c). The D, E, F and G emission components are located at 706 nm ($\sim 14164 \text{ cm}^{-1}$), 765 nm ($\sim 13060 \text{ cm}^{-1}$), 732 nm ($\sim 13650 \text{ cm}^{-1}$) and 841 nm ($\sim 11887 \text{ cm}^{-1}$), respectively. From the literatures, some researchers claimed that these peaks in the NIR emission region might be originated from the PL emission bands of MgO or Ta₂O₅ or defect states, e.g., oxygen vacancies [18-20].

The visible light (near blue light) emission in the wide band gap materials can be explained by the recombination process of the electrons. Defects such as oxygen vacancies in the lattice can promote the population of trapped electrons that induce the recombination process. Note that the optical band gap energy of SLMTO is reported to be 4.5-5.0 eV and SLMTO belongs to the wide band gap oxide materials. However, understanding the microscopic origin of the enhanced NIR emission is not clear yet.

To shed light on the increase of defects related to TaO₆ octahedral in the SLMTO powders, we measured the x-ray absorption spectroscopy (XAS) for SLMTO samples sintered at 1200°C and 1400°C, respectively. Fig. 4(a) shows the Ta L₃-edge (near 9.881 keV) XAS spectra for both of SLMTO powders. The black line and red line represent the SLMTO samples sintered at 1400°C and 1200°C, respectively. The peaks (denoted by A and B) of the XAS spectra in the two samples do not show any significant change, specifically near the absorption edge, as shown in Fig. 4(a). Note that these two peaks are associated with the *t*_{2g} and *e*_g final states, split by the crystal field effect. The relative intensity of *A* and *B* peaks results from the number of *d* electrons and hole. The XAS data indicates that the oxidation state of Ta is almost identical with +5 in the both of SLMTO samples [21].

To obtain the clear experimental evidence in the modulation of defect states, we adopted new advanced x-ray technique, resonant inelastic x-ray scattering (RIXS), as shown in Fig. 4(b) and 4(c). In the RIXS setup, we use an energy-tuned incident photon energy, which is resonate with L₃ absorption edge of specific Ta element. This photon can promote a core electron into an empty valence state. Due to the core hole, the system becomes unstable and subsequently a different occupied Ta 5d electron decays, annihilating the 2p core hole. At the end of this second order scattering process, electronic excitation between 5d orbitals are created. The difference in x-ray photon energy between incident and emission is called to energy loss (or energy transfer) and it can directly explore the electronic structure properties. Ta in stoichiometric SLMTO has 5+ valency and 5d orbitals are fully unoccupied (5d⁰). When oxygen vacancies related to Ta ion exist, 5d orbitals become partially occupied. We can probe Ta 5d-related defects state inside the band gap of SLMTO by RIXS at the Ta L₃-absorption edge. Technical point of view, RIXS is a unique powerful tool to

monitor the band gap and detect element-specific defect states inside the band gap of SLMTO.

Fig. 4(b) and (c) show the high resolution Ta L_3 -edge RIXS spectra as functions of the incident photon energy (E_i) for SLMTO powders sintered at 1200 °C and 1400 °C, respectively. The vertical line of intensity at zero energy loss is denoted by the elastic peak. The broad excitation peaks at around 9 eV resonantly enhanced when E_i is tuned near the primary XAS peak. The RIXS spectra can reveal the overall structure of the unoccupied states and band gap of SLMTO samples. Fig. 5 (the inset of Fig. 5) shows the clear band gap (4.5 – 5 eV). No existence of observable peak below the band gap in Fig. 4(b), Fig. 4(c), and Fig. 5 clearly specifies that there is little and negligible Ta-related defect in the both samples for the formation of Ta 5d states. Remarkably, the amount of Ta-related defect states in the SLMTO sample sintered at 1400°C are nearly same with that of the sample sintered at 1200°C. Therefore, we can claim that the Ta-related defects could not be correlated with the enhanced NIR region in the PL spectra. For the microscopic origin of enhanced NIR region, we rule out the possibility of Ta-related defects scenario but still need further studies in order to resolve other possibilities, e.g., other defects which is not related to Ta ion.

4. Conclusion

In summary, we investigated structural and photoluminescence (PL) properties of SrLaMgTaO₆ (SLMTO) double perovskite powder samples sintered at different temperatures (1200°C and 1400°C) for white light emitting device (LED) application. All corresponding XRD peaks in the both SLMTO samples were well indexed to a monoclinic double perovskite structure with P21/n space group. We observed quite different PL spectra in the two SLMTO samples; the PL spectra of the sample sintered at higher temperature (1400°C) exhibit suppressed blue light region and the increase of near infrared (NIR) region, compared with that of the sample at lower temperature (1200°C). To examine the scenario of Ta-related defects, we performed x-ray absorption spectroscopy and resonant inelastic x-ray scattering. RIXS results clearly show little amount of Ta-related defect in the both samples and the weak relationship between the Ta-related defects and enhancement of the PL spectra.

Acknowledgments

The use of the Advanced Photon Source at the Argonne National Laboratory was supported by the US DOE under Contract No. DE-AC02-06CH11357. This work was supported by a Research Grant of Pukyong National University in 2016.

Figure Captions

Figure 1 | X-ray diffraction (XRD) θ - 2θ scan measurements and Rietveld of SrLaMgTaO₆ (SLMTO) powder samples sintered at different temperatures. (a) Temperature-dependence of SLMTO growth: 1200 °C (up) and 1400 °C (bottom). (b) Schematic of crystal structure of SLMTO double perovskite structure.

Figure 2 | Chemical and morphological properties of SLMTO. (a) Energy-dispersive x-ray spectra (EDS) of SLMTO powder sintered at 1200°C. (b) EDS of the sample sintered at 1400°C. The insets show scanning electron microscopic image with 1 mm scale bar.

Figure 3 | Photoluminescence (PL) spectra of SLMTO powder. (a) The PL spectra of both samples sintered at 1200°C (blue) and 1400°C (red). (b) PL spectra with fitted and decomposed peaks of SLMTO samples sintered at (b) 1200°C and (c) 1400°C. Open black circles represent measured spectra, with fitted spectra and decomposed peaks represented by red solid line and dashed line, respectively.

Figure 4 | X-ray absorption spectroscopy (XAS) and resonant inelastic x-ray scattering (RIXS). (a) Ta L₃-edge XAS spectra of SLMTO powder samples: 1200°C (red) and 1400°C (black). (b) RIXS spectra of SLMTO samples sintered at (b) 1200°C and (c) 1400°C as a function of the incident photon energy and energy loss.

Figure 5 | Ta L₃-edge RIXS spectra. The RIXS spectra of SLMTO sintered at 1200°C (red line) and 1400°C (black line). The inset shows same RIXS spectra with the logarithmic y-scale.

References

References

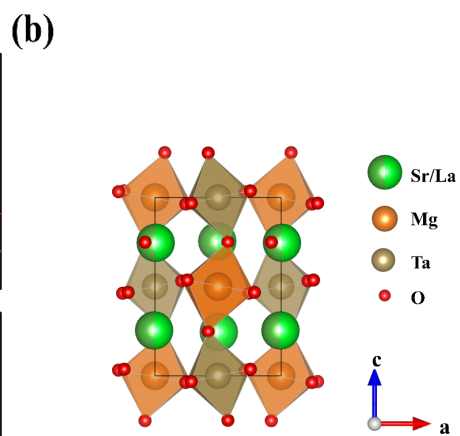
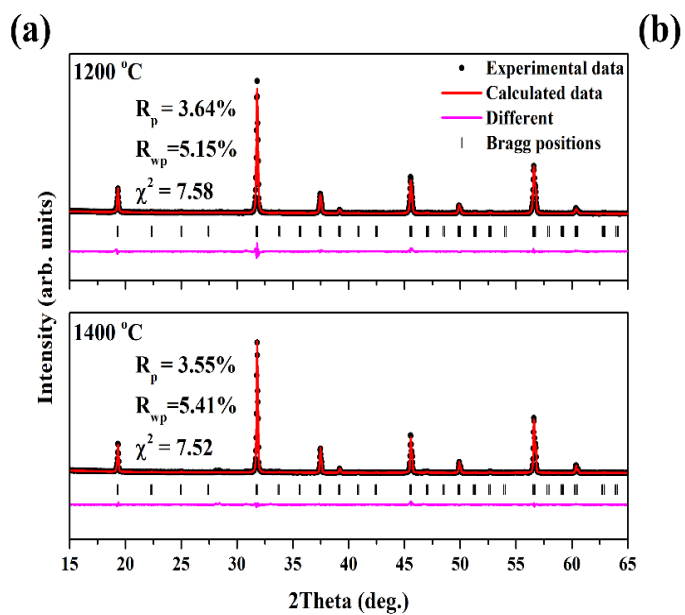
- [1] I.H. Cho, G. Anoop, D.W. Suh, S.J. Lee, J.S. Yoo, On the stability and reliability of $\text{Sr}_{1-x}\text{Ba}_x\text{Si}_2\text{O}_2\text{N}_2:\text{Eu}^{2+}$ phosphors for white LED applications, *Opt. Mater. Express.* 2 (2012) 1292.
- [2] R. Praveena, L. Shi, K.H. Jang, V. Venkatramu, C.K. Jayasankar, H.J. Seo, Sol-gel synthesis and thermal stability of luminescence of $\text{Lu}_3\text{Al}_5\text{O}_{12}:\text{Ce}^{3+}$ nano-garnet, *J. Alloys Compd.* 509 (2011) 859–863.
- [3] C. Shen, C. Zhong, J. Ming, $\text{YAG}:\text{Ce}^{3+}$, Gd^{3+} nano-phosphor for white light emitting diodes, *J. Exp. Nanosci.* 8 (2013) 54–60.
- [4] Y. Hu, W. Zhuang, H. Ye, D. Wang, S. Zhang, X. Huang, A novel red phosphor for white light emitting diodes, *J. Alloys Compd.* 390 (2005) 226–229.
- [5] T. Senden, E.J. van Harten, A. Meijerink, Synthesis and narrow red luminescence of $\text{Cs}_2\text{HfF}_6:\text{Mn}^{4+}$, a new phosphor for warm white LEDs, *J. Lumin.* 194 (2018) 131–138.
- [6] Y. Guo, B. Kee Moon, S. Heum Park, J. Hyun Jeong, J. Hwan Kim, K. Jang, R. Yu, A red-emitting perovskite-type $\text{SrLa}_{(1-x)}\text{MgTaO}_6:\text{Eu}^{3+}$ for white LED application, *J. Lumin.* 167 (2015) 381–385.
- [7] D.R. Kim, S.W. Park, B.K. Moon, S.H. Park, J.H. Jeong, H. Choi, J.H. Kim, The role of Yb^{3+} concentrations on Er^{3+} doped SrLaMgTaO_6 double perovskite phosphors, *RSC Adv.* 7 (2017) 1464–1470.
- [8] Y. Il Kim, P.M. Woodward, Crystal structures and dielectric properties of ordered double perovskites containing Mg^{2+} and Ta^{5+} , *J. Solid State Chem.* 180 (2007) 2798–2807.
- [9] S. Kato, E. Ohmorit, Y. Suzuki, Y. Ohshima, M. Sugai, H. Takizawa, T. Endo, Cation Ordering in the Oxygen Deficient Perovskite $\text{Sr}_{2-x}\text{La}_x\text{Mg}_{1-y}\text{Ta}_{1+y}\text{O}_z$, *J. Ceram. Soc. Japan.* 107 (1999) 209–214.
- [10] S. H. Chang, Y. J. Chang, S. Y. Jang, D. W. Jeong, C. U. Jung, Y.-J. Kim, J.-S. Chung, T. W. Noh, Thickness-dependent structural phase transition of strained SrRuO_3 ultrathin films: the role of octahedral tilt, *Phys. Rev. B* 84 (2011) 104101.
- [11] S. H. Chang, N. Danilovic, K.-C. Chang, R. Subbaraman, A. P. Paulikas, D. D. Fong, M. J. Highland, P. M. Baldo, V. R. Stamenkovic, J. W. Freeland, J. A. Eastman, N. M. Markovic, Functional links between stability and reactivity of strontium ruthenate single crystals during oxygen evolution, *Nat. Commun.* 5 (2014) 4191.

- [12] L.J.P. Ament, M. van Veenendaal, T.P. Devereaux, J.P. Hill, J. van den Brink, Resonant inelastic x-ray scattering studies of elementary excitations, *Rev. Mod. Phys.* 83 (2011) 705–767.
- [13] M. Y. Jeong, S. H. Chang, B. H. Kim, J.-H. Sim, A. Said, D. Casa, T. Gog, E. Janod, L. Cario, S. Yunoki, M. J. Han, J. Kim, Direct experimental observation of the molecular $J_{\text{eff}} = 3/2$ ground state in the lacunar spinel GaTa_4Se_8 , *Nat. Commun.* 8 (2017) 782.
- [14] B.H. Toby, R factors in Rietveld analysis: How good is good enough?, *Powder Diffr.* 21 (2006) 67–70.
- [15] J.Y. Park, J.S. Joo, H.K. Yang, M. Kwak, Deep red-emitting $\text{Ca}_{14}\text{Al}_{10}\text{Zn}_6\text{O}_{35}:\text{Mn}^{4+}$ phosphors for WLED applications, *J. Alloys Compd.* 714 (2017) 390–396.
- [16] W. Ran, H.M. Noh, B.K. Moon, S.H. Park, J.H. Jeong, J.H. Kim, G. Liu, J. Shi, Crystal structure, electronic structure and photoluminescence properties of $\text{KLaMgWO}_6:\text{Eu}^{3+}$ phosphors, *J. Lumin.* 197 (2018) 270–276.
- [17] T. Horikubi, H. Watanabe, N. Kamegashira, Structure of perovskite type compounds, ALaMnTaO_6 (A=Sr, Ba), *J. Alloys Compd.* 274 (1998) 122–127.
- [18] N. Jain, N. Marwaha, R. Verma, B.K. Gupta, A.K. Srivastava, Facile synthesis of defect-induced highly-luminescent pristine MgO nanostructures for promising solid-state lighting applications, *RSC Adv.* 6 (2016) 4960–4968.
- [19] N. Pathak, P.S. Ghosh, S.K. Gupta, R.M. Kadam, A. Arya, Defects induced changes in the electronic structures of MgO and their correlation with the optical properties: a special case of electron–hole recombination from the conduction band, *RSC Adv.* 6 (2016) 96398–96415.
- [20] H. Shin, S.Y. Park, S.T. Bae, S. Lee, K.S. Hong, H.S. Jung, Defect energy levels in Ta_2O_5 and nitrogen-doped Ta_2O_5 , *J. Appl. Phys.* 104 (2008) 5–7.
- [21] T.K. Mandal, V. V. Poltavets, M. Croft, M. Greenblatt, Synthesis, structure and magnetic properties of $\text{A}_2\text{MnB}'\text{O}_6$ (A=Ca, Sr; B'=Sb, Ta) double perovskites, *J. Solid State Chem.* 181 (2008) 2325–2331.

Table I.

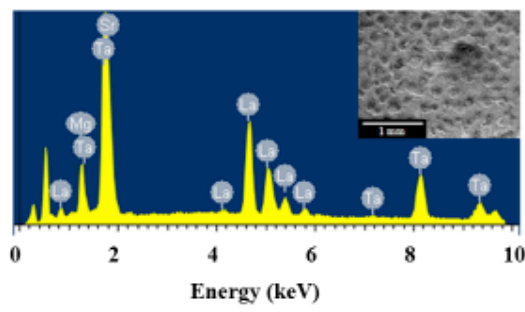
Lattice parameters obtained from Rietveld refinement of XRD pattern for SrLaMgTaO₆ powders.

SrLaMgTaO ₆		
	1200 °C	1400 °C
a (Å)	5.639	5.635
b (Å)	5.629	5.639
c (Å)	7.958	7.965
α (°)	90	90
β (°)	89.98	90.01
γ (°)	90	90
V (Å ³)	252.6	253.1

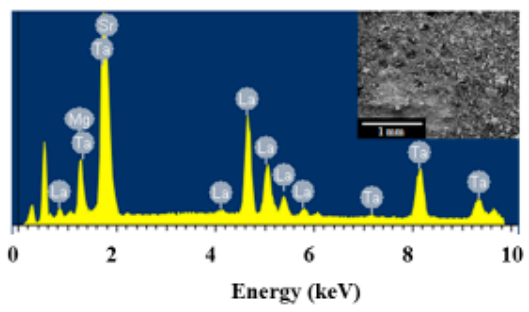


Oh *et al.*, Fig. 1.

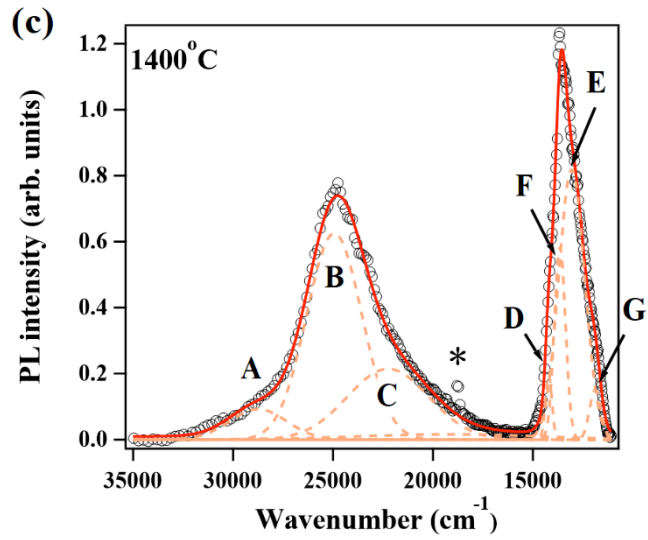
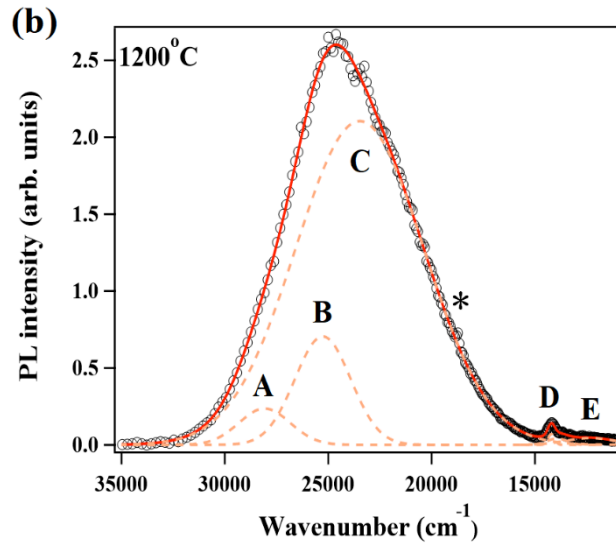
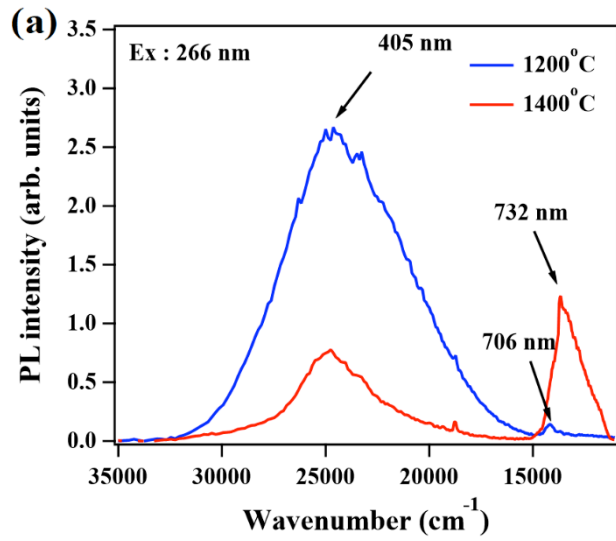
(a) 1200 °C



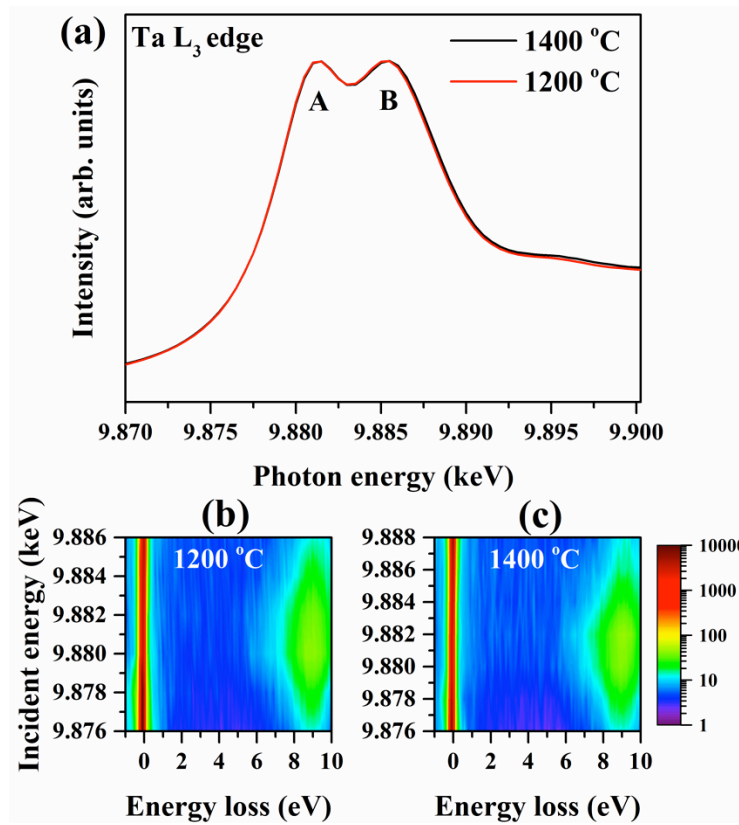
(a) 1400 °C



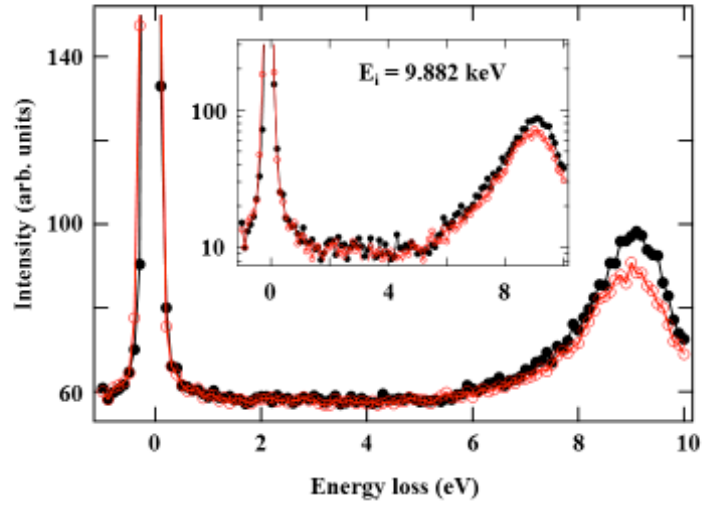
Oh *et al.*, Fig. 2.



Oh *et al.*, Fig. 3.



Oh *et al.*, Fig. 4.



Oh *et al.*, Fig. 5.